Research on the Design Method of Tunnel Vibration Isolation Layer Based on Stiffness-Damping Coupling

Yuang Shan

Lanzhou Jiaotong University, Lanzhou 730070, China

syangive@163.com

Abstract. The construction of the western tunnel inevitably encounters the problem of seismic isolation design in high-intensity seismic zones. However, the current anti-seismic calculation methods applicable to tunnel structures mostly adopt the static method and simply increase the stiffness, resulting in overly conservative calculation results and failure to consider the coordinated deformation between tunnel structures. The seismic isolation effect is generally poor. Considering the coordinated deformation between tunnel structures, that is, the coupling effect of stiffness and damping, and taking the generalized composite structure of the tunnel as the object, based on the dynamic equation, integrating the equation relationships of stiffness-damping and other constant parameters, a tunnel seismic isolation layer design method that can achieve precise calculation of stiffness-damping is proposed. Through the calculation of actual engineering cases, this method can solve the optimal values of stiffness-damping of the seismic isolation layer, ensuring that the amplitude of the seismic response of the tunnel structure is minimized under the action of earthquakes. This is of great significance for guiding the selection and design of tunnel seismic isolation layer materials.

Keywords: Tunnel engineering, Seismic isolation design, Stiffness, Damping, Calculation method.

1 Introduction

With the implementation of the Western Development Strategy, tunnel construction in high-intensity seismic zones of Western China has increased significantly, bringing the issue of seismic damage in these tunnels to the forefront[1-2]. Currently, tunnel engineering often employs the method of installing vibration isolation layers to reduce the seismic response of tunnel structures. However, the prevailing design methods for these layers are qualitative and singular, primarily considering only the stiffness factor of the isolation layer while neglecting the mismatch between the stiffness-damping coupling parameters of the isolation layer and those of the primary and secondary linings[3-4]. This oversight leads to suboptimal seismic isolation performance, making it difficult to effectively address the diverse seismic challenges in Western regions. Therefore, there is an urgent need for a design method for vibration isolation layers under seismic action

© The Author(s) 2026
S. Sing et al. (eds.), *Proceedings of the 2025 7th International Conference on Civil Architecture and Urban Engineering (ICCAUE 2025)*, Atlantis Highlights in Engineering 43,
https://doi.org/10.2991/978-94-6239-682-1_21

that considers the stiffness-damping coupling of tunnel structures. Such a method would enable the precise determination of the design range for isolation layer stiffness and damping, achieving optimal matching of stiffness-damping parameters among all structural layers. This ensures the deformation compatibility relationship between tunnel layers and achieves effective seismic isolation.

2 Generalized Composite Structure Stiffness-Damping Matching Control Equation

2.1 Basic Assumptions

Based on the interaction characteristics between the tunnel and surrounding rock, and considering the structural features of the tunnel, a generalized composite structure of "surrounding rock–primary lining–isolation layer–secondary lining" is proposed. The following basic assumptions are made for this generalized composite structure:

(1) Taking the tunnel vibration isolation layer as the research object, an isolation body comprising partial surrounding rock, primary lining, isolation layer, and secondary lining is considered, and all are treated as homogeneous, elastoplastic media.

(2) The longitudinal length of the tunnel is much greater than its cross-sectional dimensions; therefore, the generalized composite structure is modeled considering a plane strain stress state.

(3) Considering the instantaneous-reciprocal characteristics of seismic action, the interfaces between layers in the generalized composite structure are in close contact, connected in a viscoelastic manner[5-6], exhibiting instantaneous deformation, elastic aftereffect, and stress relaxation characteristics. The surrounding rock, primary lining, isolation layer, secondary lining, and their interlayer interfaces collectively constitute the generalized composite structure mechanical model.

2.2 Mechanical Model

Following the plane strain stress state, an isolation body comprising partial surrounding rock, primary lining, isolation layer, and secondary lining is extracted to construct a physical model of the generalized composite structure. Seismic loading, characterized by tension-compression cycles, exhibits instantaneous-reciprocal properties. Each isolation body is considered a homogeneous, elastoplastic medium, with failure occurring when plastic deformation exceeds a certain limit. Consequently, the interlayer interface model is selected as the Poynting-Thomson mechanical model[7] (see Fig. 1), based on its characteristics of instantaneous deformation, elastic aftereffect, and stress relaxation. According to the basic assumptions, the isolation bodies and their interlayer interfaces together form the generalized composite structure mechanical model (see Fig. 2).

$$\sigma' + \frac{k_1}{c}\sigma = \left(k_1 + k_2\right)\varepsilon' + \frac{k_1 k_2}{c}\varepsilon \tag{1}$$

Simplifying the constitutive equation under constant load conditions yields:

$$\sigma = k_2\varepsilon_2 + c\frac{(k_1+k_2)}{k_1}\varepsilon' \tag{2}$$

Combining the constitutive equations of the Maxwell body and the elastic element, the constitutive equation of the Poynting-Thomson body can be further transformed as follows:

$$\begin{cases} \sigma_1 = \dfrac{(k_1+k_2)}{k_1}c\varepsilon' \\ \sigma_2 = k_2\varepsilon \end{cases} \tag{3}$$

Based on Equation (3), the mechanical parameters of the generalized composite structure mechanical model are defined as follows: Let the stiffness of the surrounding rock be K_1 and K_2 , damping be C_1, and mass be M_1; the stiffness of the primary lining be K_3 and K_4, damping be C_2, and mass be M_2; the stiffness of the isolation layer be K_5 and K_6, damping be C_3, and mass be M_3; the stiffness of the secondary lining be K_7 and K_8, damping be C_4, and mass be M_4.

Through the generalized composite structure mechanical model, displacement and deformation compatibility between the "surrounding rock–primary lining–isolation layer–secondary lining" is achieved. Simultaneously, it is evident that the displacement and deformation compatibility of each structure is closely related to its stiffness and damping.

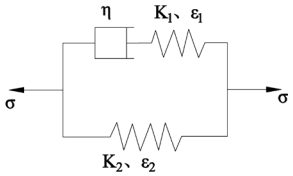

Fig. 1. Poynting-Thomson body mechanical model

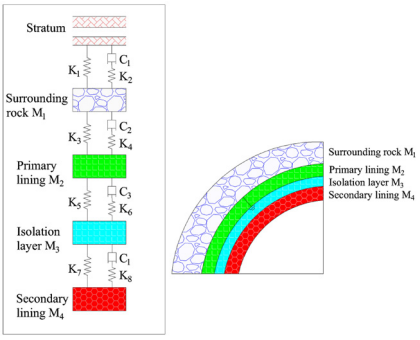

Fig. 2. Generalized composite structure mechanical model

2.3 Dynamic Equations

Under seismic action, each isolation body generates a seismic response displacement. A smaller seismic response displacement of the tunnel structure can be interpreted as smaller deformation produced by the structure, indicating greater safety.

Let the base seismic input displacement Z_0 cause absolute displacements of the surrounding rock M_1, primary lining M_2, isolation layer M_3, and secondary lining M_4 as Z_1, Z_2, Z_3, and Z_4, respectively. Considering the relative coordinate relationship, the displacements of the "surrounding rock–primary lining–isolation layer–secondary lining" relative to the base are established as:

$$\begin{cases} U_1 = Z_1 - Z_0 \\ U_2 = Z_2 - Z_0 \\ U_3 = Z_3 - Z_0 \\ U_4 = Z_4 - Z_0 \end{cases} \tag{4}$$

As shown in Fig. 2, force analysis is conducted on each isolation body using the constitutive equation of the Poynting-Thomson mechanical model and the strength theory of generalized Hooke's law to determine the forces on the "surrounding rock–primary lining–isolation layer–secondary lining":

$$\begin{cases} \begin{cases} f_1 = K_1\left(Z_1 - Z_0\right) = K_1 U_1 \\ f_2 = \dfrac{K_1 + K_2}{K_2} C_1 U_1' = \rho_1 C_1 U_1' \end{cases} \\ \begin{cases} f_3 = K_3\left(Z_2 - Z_1\right) = K_3\left(U_2 - U_1\right) \\ f_4 = \dfrac{K_3 + K_4}{K_4} C_2\left(U_2' - U_1'\right) = \rho_2 C_2\left(U_2' - U_1'\right) \end{cases} \\ \begin{cases} f_5 = K_5\left(Z_3 - Z_2\right) = K_5\left(U_3 - U_2\right) \\ f_6 = \dfrac{K_5 + K_6}{K_6} C_3\left(U_3' - U_2'\right) = \rho_3 C_2\left(U_3' - U_2'\right) \end{cases} \\ \begin{cases} f_7 = K_7\left(Z_4 - Z_3\right) = K_7\left(U_4 - U_3\right) \\ f_8 = \dfrac{K_7 + K_8}{K_8} C_4\left(U_4' - U_3'\right) = \rho_4 C_4\left(U_4' - U_3'\right) \end{cases} \end{cases} \tag{5}$$

Based on Equation (4), the equilibrium equations for each isolation body of the "surrounding rock–primary lining–isolation layer–secondary lining" are constructed as follows:

$$\begin{cases} \sum F_1 = -f_1 - f_2 + f_3 + f_4 = M_1 Z_1'' = M_1\left(U_1'' + Z_0''\right) \\ \sum F_2 = -f_3 - f_4 + f_5 + f_6 = M_2 Z_2'' = M_2\left(U_2'' + Z_0''\right) \\ \sum F_3 = -f_5 - f_6 + f_7 + f_8 = M_3 Z_3'' = M_3\left(U_3'' + Z_0''\right) \\ \sum F_4 = -f_7 - f_8 + f_9 + f_{10} = M_4 Z_4'' = M_4\left(U_4'' + Z_0''\right) \end{cases} \tag{6}$$

Considering the stiffness compatibility relationship of the "surrounding rock–primary lining–isolation layer–secondary lining", and observing that the equation system (6) shares a common component $\frac{K_{2i-1}+K_{2i}}{K_{2i}}$ with the constitutive equation (3) of the Poynting-Thomson mechanical model, which is closely related to the stiffness of the isolation body, this component is defined as the dynamic stiffness matching basis ρ_i characterizing the stiffness properties of the isolation body. Combining with the constitutive equation (3) of the Poynting-Thomson mechanical model, it can be inferred that when the stress on the isolation body exceeds the critical state, interface relaxation occurs. In reality, this corresponds to detachment or failure of the tunnel structure, where stiffness ceases to function, and ρ=1 at this point.

To simplify the calculation, assuming consistent interface behavior across all structures, let $\rho_1=\rho_2=\rho_3=\rho_4$. Combining Equations (4), (5), and (6), a four-degree-of-freedom vibration system dynamic calculation model is constructed:

$$[M]\{U''\}+[\rho][C]\{U'\}+[K]\{U\}=\{F_e\} \tag{7}$$

This dynamic calculation model can be expanded as:

$$\begin{bmatrix} M_1 & 0 & 0 & 0 \\ 0 & M_2 & 0 & 0 \\ 0 & 0 & M_3 & 0 \\ 0 & 0 & 0 & M_4 \end{bmatrix}\begin{bmatrix} U_1'' \\ U_2'' \\ U_3'' \\ U_4'' \end{bmatrix}+\begin{bmatrix} \rho_1 & 0 & 0 & 0 \\ 0 & \rho_2 & 0 & 0 \\ 0 & 0 & \rho_3 & 0 \\ 0 & 0 & 0 & \rho_4 \end{bmatrix}\begin{bmatrix} C_1+C_2 & -C_2 & 0 & 0 \\ -C_2 & C_2+C_3 & -C_3 & 0 \\ 0 & -C_3 & C_3+C_4 & -C_4 \\ 0 & 0 & -C_4 & C_4 \end{bmatrix}\begin{bmatrix} U_1' \\ U_2' \\ U_3' \\ U_4' \end{bmatrix}$$
$$+\begin{bmatrix} K_1+K_3 & -K_3 & 0 & 0 \\ -K_3 & K_3+K_5 & -K_5 & 0 \\ 0 & -K_5 & K_5+K_7 & -K_7 \\ 0 & 0 & -K_7 & K_7 \end{bmatrix}\begin{bmatrix} U_1 \\ U_2 \\ U_3 \\ U_4 \end{bmatrix}=\begin{bmatrix} -M_1Z_0'' \\ -M_2Z_0'' \\ -M_3Z_0'' \\ -M_4Z_0'' \end{bmatrix} \tag{8}$$

The value of the dynamic stiffness matching basis ρ_i is determined as follows:

$$\rho_i=\begin{cases} \dfrac{K_{2i-1}+K_{2i}}{K_{2i}}, \text{ When } \sigma\le\sigma_s, \text{ the working state} \\ 1, \text{ When} \sigma>\sigma_s, \text{ reaching the limit, destruction} \end{cases} \tag{9}$$

σ_s ------Critical stress state of the interface model.

Analysis shows that Matrix (7) is in the form of an implicit function. The masses of the isolation bodies are constants. The relative displacement U, seismic response velocity U', and acceleration U'' of the isolation bodies, which reflect the vibration reduction effect, are all related to their stiffness and damping. If the implicit function matrix (7) is solved, i.e., expressing the displacement representing the vibration reduction effect as an explicit function of stiffness K and damping C, a design method for the isolation layer determined by stiffness-damping, based on the standard of isolation layer displacement response, can be established.

2.4 Solution of the Dynamic Calculation Model

Therefore, Matrix (7) is solved using the implicit function theorem and differentiation methods.

In the complex function domain, the base seismic input displacement is:

$$Z_0 = A_0\left(\cos\omega t + i\sin\omega t\right) = A_0 e^{i\omega t} \tag{10}$$

The solution of the dynamic calculation model is assumed to be:

$$\left[U\right] = \left[X(t)\right] = \left[X\right]e^{i\omega t} \tag{11}$$

From Equations (10) and (11), it can be derived that:

$$Z_0^{"} = -A_0\omega^2\left[\cos\omega t + i\sin\omega t\right] \tag{12}$$

$$\left[X'(t)\right] = i\omega\left[X\right]e^{i\omega t} \tag{13}$$

$$\left[X^{"}(t)\right] = -\omega^2\left[X\right]e^{i\omega t} \tag{14}$$

Substituting Equations (10)-(14) into the dynamic calculation model yields:

$$-\omega^2\left[M\right]\left[X\right]e^{i\omega t} + i\omega\left[C\right]\left[X\right]e^{i\omega t} + \left[K\right]\left[X\right]e^{i\omega t} = \left[F_M\right]e^{i\omega t} \tag{15}$$

Let:

$$\begin{aligned}\left[S(\omega)\right] &= -\omega^2\left[M\right] + i\omega\left[\rho\right]\left[C\right] + \left[K\right]\\ \left[F_M\right] &= \left[M\right]A_0\omega^2\end{aligned} \tag{16}$$

Equation (15) can be simplified to:

$$\left[S(\omega)\right]\left[X\right] = \left[F_M\right] \tag{17}$$

Assuming the seismic excitation frequency ω is not a solution of $\left|\left[S(\omega)\right]\right| = 0$, solving the dynamic calculation model (17) yields:

$$\left[X\right] = \left[S(\omega)\right]^{-1}\left[F_M\right] \tag{18}$$

Solution (18) is the result of solving the implicit function matrix (7), i.e., the explicit form of the implicit function (7). Solution (18) is the complex amplitude sought for the system. According to complex number operation rules, the real amplitude of the system can be obtained. X_3 represents the vibration reduction response displacement of the isolation layer.

Since the mass of each isolation body is not the primary focus, for the seismic response displacement of the isolation layer, Let $M_1 = m$, $M2 = \alpha m$, $M_3 = \beta m$, $M_4 = \gamma m$. Simplifying Equation (13) yields:

$$X_3 = A_0 m\omega^2 \left\{ \left[S(\omega) \right]^{-1} \left[M' \right] \right\}_{(3,1)} \tag{19}$$

2.5 Vibration Isolation Stiffness-Damping Matching Calculation

The seismic response displacement of each isolation body does not intuitively demonstrate the vibration reduction effect. Therefore, the ratio of the isolation body's seismic response displacement to the input displacement is adopted to visually represent the reduction effect. A smaller ratio indicates better vibration reduction performance of the isolation layer.

To reflect the forced vibration response of the isolation layer, the complex-plane seismic response amplitude ratio function *D3* of the isolation layer is constructed to characterize the ratio of the maximum complex amplitude of the forced vibration response of the tunnel isolation layer to the base input displacement amplitude *A0*:

$$D_3 = \frac{X_3}{A_0} = m\omega^2 \left\{ \left[S(\omega) \right]^{-1} \left[M' \right] \right\}_{(3,1)} \tag{20}$$

Considering the decoupling of stiffness and damping in the generalized composite structure, the complex-plane seismic response amplitude ratio function of the isolation layer (15) is organized in the real plane as follows:

$$\left| D_3 \right| = \left| \frac{X_3}{A_0} \right| = m\omega^2 \sqrt{\frac{\left(O_1 K_5 + P_1 C_3 + Q_1 \right)^2 + \left(O_2 K_5 + P_2 C_3 + Q_2 \right)^2}{\left(R_1 K_5 + S_1 C_3 + T_1 \right)^2 + \left(R_2 K_5 + S_2 C_3 + T_2 \right)^2}} \tag{21}$$

where the constants O, P, Q, R, S, T contain parameters such as α, β, γ, C_i (i=1, 2, 4), ρ_i (i=1, 2, 3, 4), K_i(i=1, 3, 7), ω.

Here, α, β, γ are the mass ratios of the isolation body units for each tunnel layer, which are determined constants; ω is the frequency of the local earthquake, a constant. Analysis shows that for different stiffness *K* and damping *C*, the tunnel isolation layer seismic response amplitude ratio function has a uniquely determined corresponding value on the real plane.

Geometrically, when constants such as *α, β, γ, ω, ρi* are determined, a spatial surface composed of coordinates formed by the seismic response amplitude D_3, stiffness *K*, and damping *C* can be defined. All values on this surface are known. Therefore, this surface can guide the design of the tunnel isolation layer to achieve optimal vibration reduction.

3 Case Study Analysis

3.1 Engineering Background

Taking a tunnel in Sichuan Province as the engineering prototype, the site is surrounded by multiple developed faults with the potential to generate earthquakes of approximately magnitude 7. The primary lining of the tunnel uses 24.00 cm thick C20 shotcrete, and the secondary lining uses 50.00 cm thick C30 reinforced concrete. The designed peak ground acceleration is 0.35g for a magnitude 7 earthquake. The unit thickness of surrounding rock participating in the calculation is 60.00 cm, the isolation layer thickness is set to 20.00 cm, and the unit weight is 15.00 kN/m³. The tunnel employs a composite lining with an arched cross-section.

The main material calculation parameters for the tunnel body are shown in Table 1.

The model uses frequency-independent Local damping to approximately characterize the damping effect of the rock and soil during seismic wave propagation. Based on experience, the damping for the lining structure is taken as 0.10, and for the surrounding rock as 0.20. The specific material parameters are listed in Table 1[8].

Table 1. Main Physical and Mechanical Parameters of Materials

Material	Thickness b(cm)	Unit Weight P(kN/m^3)	Elastic Modulus E(GPa)	Poisson's Ratio υ	Cohesion c (MPa)	Friction Angle (°)	Damping C (N·s/m)
Surrounding Rock	60.00	20.00	6.0	0.30	-	40	0.20
Primary Lining	24.00	24.50	25.2	0.20	1.5	55	0.10
Isolation Layer	20.00	15.00	To be determined	0.30	0.6	6	To be determined
Secondary Lining	50.00	27.50	30.0	0.20	2	50	0.10

3.2 Vibration Isolation Stiffness-Damping Matching Calculation

The coefficients in the isolation layer seismic response amplitude ratio function (16) are determined using the following equations:

$$M = \rho \times blt \tag{22}$$

$$K = \frac{Eb^3 t}{4l^3} \tag{23}$$

$$M_L = \lg A_0 + R(\triangle) \tag{24}$$

$$Z_0'' = -A_0\omega^2 e^{i\omega t} \tag{25}$$

In the equations, M~L~ is the local magnitude (near earthquake magnitude), A_0 is the arithmetic mean of the maximum ground displacements recorded in two horizontal components (μm), and R(Δ) is the calibration function for short-period seismometers commonly used in China to determine M_L, assigned values based on relevant experience[9].

Using Equations (22)-(25) and the explicit function form solution (21), the isolation layer seismic response amplitude ratio function can be solved as:

$$|D_3| = 1200 \times 0.59^2 \times \sqrt{\frac{(40.3567K_5 - 20480.05461C_3 - 3390.613079)^2 + (104134.5K_5 + 7.9369C_3 - 5368100.001)^2}{(-16361.3466K_5 + 8567729.715C_3 + 1416287.693)^2 + (-43567698.57K_5 - 3217.695597C_2 + 2242350774)^2}} \tag{26}$$

Based on experience, the value ranges for E_5 and D_3 in Equation (22) are determined as[10-11]:

$$0.5MPa \le E_5 \le 5000MPa$$
$$0.01N \cdot s/m \le C_3 \le 0.35N \cdot s/m$$

The numerical distribution in the $|D_3|$-K_5-C_3 three-dimensional space is solved. Substituting dimensionless stiffness and using MATLAB, the numerical distribution of $|D_3|$-K_5-C_3 within the specified region is determined (see Fig. 3). Figure 3 represents the aforementioned spatial surface composed of coordinates formed by the seismic response amplitude D_3, stiffness K, and damping C.

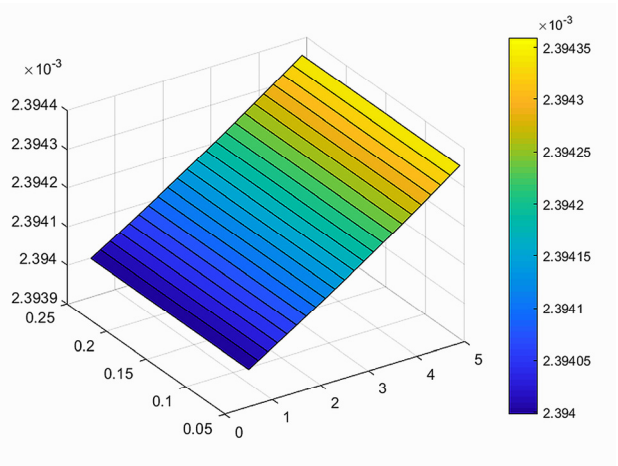

Fig. 3. Numerical distribution in $\frac{|D_3|}{1200 \times 0.59^2}$-$K_5$-$C_3$ three-dimensional space

The vertical coordinate in the figure represents the value of $\frac{|D_i|}{1200 \times 0.59^2}$. A smaller value indicates a smaller real amplitude of forced vibration in the isolation layer and better vibration isolation effect.

(2) Using MATLAB, the optimal solution for the forced vibration response function in this case study is calculated as:

$$K_5=0.5017\text{GPa},\ C_3=0.1918\text{N}\cdot\text{s/m}$$

At these values, the displacement transfer coefficient of the isolation layer's forced vibration is minimized, meaning the real amplitude of forced vibration is smallest, resulting in the best vibration isolation effect.

In practical engineering design, constrained by material science, it is difficult to find isolation layer materials that exactly meet both the optimal stiffness *K* and damping *C*. Since this vibration reduction design method uses the seismic response displacement amplitude ratio as the design criterion, the stiffness-damping coupling design method can, based on existing isolation layer materials, compare the vibration reduction effects of different materials by determining their stiffness *K* and damping *C*, thereby identifying a more suitable vibration reduction material for the current engineering conditions.

4 Conclusion

Considering the coordinated deformation among tunnel structural components and based on dynamic equations, this study investigated the stiffness-damping coupling relationship among surrounding rock, primary lining, isolation layer, and secondary lining. Using the ratio of the tunnel vibration isolation structure's response displacement to the seismic input displacement as the design criterion, a precise design method for vibration isolation structure stiffness-damping coupling was proposed. This method considers the influence of stiffness-damping on vibration reduction, improving upon the current design approach that considers only stiffness. Based on the design parameters of a tunnel in Sichuan Province and applying this method, the optimal design parameters for the isolation layer stiffness and damping suitable for this tunnel were solved. The parameters indicate that when the isolation layer stiffness *K* is around 0.5017 G*Pa* and damping *C* is around 0.1918N·s/m, the tunnel's vibration reduction effect is optimal, demonstrating the feasibility of this design method. Furthermore, for existing vibration reduction materials, comparing their effects using this method enables visualization and efficiency in vibration reduction design, holding significant importance for guiding seismic isolation design of tunnels in Western China.

Acknowledgments

This study was supported by the Gansu Province 2025 Outstanding Graduate Student "Innovation Star" Project (Project No.: 2025CXZX-714).

References

1. Li Ming.: Research on technology for improving seismic performance of tunnel linings in high-intensity seismic zones. Technology Innovation and Application15(33),189-192 (2025)
2. Jiang Yujing, Wang Xingda, Zhang Xuepeng.: A review of seismic response research in tunnel engineering: from dynamic properties of rock mass to seismic analysis of structures. Journal of China Coal Society, 1-22(2025)
3. Lin Jinhai.: Study on seismic damage and structural safety assessment methods for railway tunnels. Railway Standard Design**10**(69),239-248+264(2025)
4. Zhang Liang, Tang Yu, Zhang Kaiwen.: Seismic vulnerability analysis of lining structures in the "slope-fault zone-tunnel" system. Advanced Engineering Sciences, 1-17(2025)
5. Mei Songhua, Sheng Qian, Cui Zhen.: Experimental study on the energy absorption characteristics of viscoelastic damping vibration isolation layers. Chinese Journal of Geotechnical Engineering**06**(44), 997-1005(2022)
6. Wen Wenlu, Yin Pengfei, Zhang Jian.: Design and application of viscous dampers in isolation layers for projects in high-intensity seismic zones. Sichuan Architecture **S1**(43), 133-137(2023)
7. Zhu Zhuohui, Zhao Yanlin, Xu Yanfei.: Teaching research on eight typical combined rheological models in rock mechanics[J]. Theory and Practice of Contemporary Education**06**(3), 85-89(2011)
8. Xu Hua, Li Tianbin.: Analysis of seismic dynamic response and vibration reduction effect of different vibration isolation layers in tunnels. China Civil Engineering Journal S1(44), 201-208(2011)
9. Chen Jifeng, Yin Xinxin, Dong Zongming, et al. Study on the calibration function of local magnitude in Gansu region. Earthquake Research in China**03**(29), 327-334(2013)
10. Hu Wenge, Yao Hui, Fu Qi.: Shaking table test study on dynamic response of the portal section of loess tunnels. China Earthquake Engineering Journal(01), 187-196(2026)
11. Ma Jianfei, Jiang Bo, Chen Zheng.: Study on the combined rigid-flexible vibration reduction effect for high-speed railway tunnels with cavities in strong earthquake zones. Journal of Safety Science and Technology20(10), 168-174(2024)

Open Access This chapter is licensed under the terms of the Creative Commons Attribution-NonCommercial 4.0 International License (http://creativecommons.org/licenses/by-nc/4.0/), which permits any noncommercial use, sharing, adaptation, distribution and reproduction in any medium or format, as long as you give appropriate credit to the original author(s) and the source, provide a link to the Creative Commons license and indicate if changes were made.

The images or other third party material in this chapter are included in the chapter's Creative Commons license, unless indicated otherwise in a credit line to the material. If material is not included in the chapter's Creative Commons license and your intended use is not permitted by statutory regulation or exceeds the permitted use, you will need to obtain permission directly from the copyright holder.